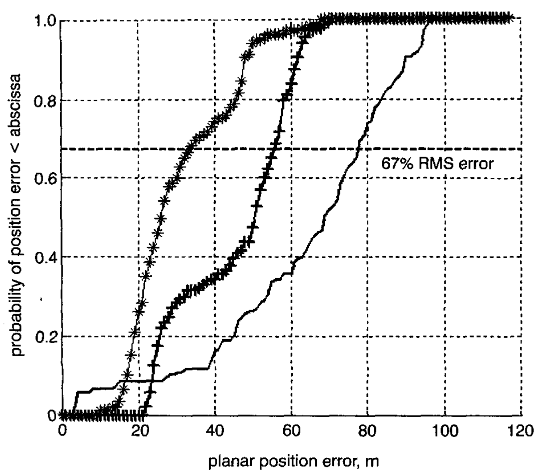

Fig. 2 *Performance comparison (empirical CDF)*
—— LS method (67% error 77.47 m)
\+ LOS reconstruction (67% error 55.56 m)
* successive bound constrained estimator (67% error 33.40 m)

Field trials were accomplished to locate an MS in the central area of Seoul. In the field trials, almost all signals received at the MS experienced NLOS propagation due to surrounding buildings and included a large bias error. Three PN sequences of signals from three neighbouring base stations were received with a specially devised terminal that can observe TOA (time of arrival) measurements. The terminal is synchronised with the GPS. Hence, the correlation of PN sequences computes the one-way propagation time of a signal. The tests were accomplished 25 times at a stationary point. The location accuracy of the LS, the LOS reconstruction method, and the proposed successive bound constrained estimator were 748, 417.45 and 110.08 m, respectively.

The proposed successive bound constrained estimator considers a feasible range of the NLOS propagation delay error, even though it may not converge to the true value. The results of this study show that doing so effectively enhances location accuracy.

Acknowledgments: The authors wish to thank Samsung Electronics, Inc., and the NRL Program of Korean Ministry of Science & Technology for their support for this work.

19 January 2002
Electronics Letters Online No: 20020726
DOI: 10.1049/el:20020726

Wuk Kim and Jang Gyu Lee (*School of Electrical Engineering and Computer Science, Seoul National University, Seoul 151-742, Korea*)

E-mail: jgl@snu.ac.kr

Gyu-In Jee (*Department of Electronic Engineering, Konkuk University, Seoul 143-701, Korea*)

ByungSoo Kim (*Samsung Electronics Inc., Suwon 442-742, Korea*)

References

1 CAFFERY, J., , JR., and STÜBER, G.L.: 'Subscriber location in CDMA cellular networks', *IEEE Trans. Veh. Technol.*, 1998, **47**, pp. 406–416
2 WYLIE, M.P., and HOLTZMANN, J.: 'The non-line-of-sight problem in mobile location estimation'. 5th IEEE Int. Conf. on Universal Personal Communication, Cambridge, MA, USA, 1996, Vol. 2, pp. 827–831
3 CHEN, P.-C.: 'A non-line-of-sight error mitigation algorithm in location estimation'. IEEE Conf. on Wireless Communications and Networking, New Orleans, LA, USA, 1999, Vol. 1, pp. 316–320
4 FOY, W.: 'Position-location solutions by taylor-series estimation', *IEEE Trans. Aerosp. Electron. Syst.*, 1976, **12**, pp. 187–193
5 'Modeling unification workshop II', COST259 TD (99) SWG 2.1, January 2000, pp. 5–9

Expression of MIMO capacity in terms of waveguide modes

P. Kyritsi and D.C. Cox

The capacity of a multiple input-multiple output system in a waveguide is expressed in terms of the waveguide modes. The number of allowable modes limits the number of equivalent spatial sub-channels. Capacity is periodic with distance along the waveguide, and depends on the mode excitation and the receiver location.

Theoretical analysis: Assume a system with M transmitters and N receivers. Each transmitter transmits an independent data stream, at power E_x. Let $\boldsymbol{x}$, $\boldsymbol{y}$ be the vectors of the transmitted/received signals, respectively. Then $\boldsymbol{y} = \mathbf{T}\boldsymbol{x} + \boldsymbol{n}$, where $\boldsymbol{n}$ is the noise vector (assumed to be additive white Gaussian noise with independent components across the receivers) and $\mathbf{T}$ is the channel transfer matrix.

The channel capacity C is given by the formula

$$C = \log_2\left(\det\left(\mathbf{I} + \frac{E_x}{\sigma^2}\mathbf{T}\mathbf{T}^{\mathrm{H}}\right)\right) \qquad (1)$$

It can be expressed in terms of the singular values λ_i of the matrix $\mathbf{T}^{\mathrm{H}}$ as

$$C = \sum_{i=1}^{K}\log_2\left(1 + \frac{E_x}{\sigma^2}\lambda_i\right) \qquad (2)$$

The channel is equivalent to K (= rank of the matrix $K \le \min(N, N)$) parallel scalar sub-channels, each of gain λ_i.

Assume a waveguide of rectangular cross-section and dimensions (a, b) as in Fig. 1. Let L be number of allowable propagating modes. The dependence of the electric field for each TE/TM mode at any location in the waveguide is given in Table 1 [1].

Table 1: Field characteristics for TE and TM modes

	TE	TM
E_x	$A_{mn}\cos((\pi m/a)x)\sin((\pi n/b)y)$	$B_{mn}\cos((\pi m/a)x)\sin((\pi n/b)y)$
E_y	$A_{mn}(na/mb)$ $\sin((\pi m/a)x)\cos((\pi n/b)y)$	$-B_{mn}(mb/na)$ $\sin((\pi m/a)x)\cos((\pi n/b)y)$

Assume a source that is excited by a sinusoid at frequency ω and let $\boldsymbol{A}$ be the vector of the resulting propagating mode coefficients at $z = 0$ (we assume that the source is placed sufficiently far from the plane $z = 0$, so that at that plane the evanescent fields have disappeared). The coefficients A_i depend on the location and polarisation of the source and are complex numbers. Under the narrowband assumption if the source were transmitting a signal of the form $g(t)\sin\omega t$, the resulting mode coefficients at the plane $z = 0$ would be $\boldsymbol{A}g(t)$. At any point (x, y, z) with $z \ge 0$, the electric field is given by:

$$E_x(x, y, z) = \sum_i A_i \cos\left(\frac{\pi m(i)}{a}x\right)\sin\left(\frac{\pi n(i)}{b}y\right)e^{jk_z(i)z} = \boldsymbol{p}_x^{\mathrm{T}}\boldsymbol{A} \qquad (3)$$

$$E_y(x, y, z) = \sum_i \delta_i A_i \sin\left(\frac{\pi m(i)}{a}x\right)\sin\left(\frac{\pi n(i)}{b}y\right)e^{jk_z(i)z} = \boldsymbol{p}_y^{\mathrm{T}}\boldsymbol{A} \qquad (4)$$

$$(\boldsymbol{p}_x)_i = \cos\left(\frac{\pi m(i)}{a}x\right)\sin\left(\frac{\pi n(i)}{b}y\right)e^{jk_z(i)z} \qquad (5)$$

$$(\boldsymbol{p}_y)_i = \delta_i \sin\left(\frac{\pi m(i)}{a}x\right)\sin\left(\frac{\pi n(i)}{b}y\right)e^{jk_z(i)z} \qquad (6)$$

The factor δ is in accordance to the type of the mode.

If we assume M sources, each one of them gives rise to a vector of the form of the vector $\boldsymbol{A}$. Let $\mathbf{A}$ be a matrix, the columns of which are those excitation vectors $\boldsymbol{A}$. If N receivers are placed at different (x, y, z) locations, let $\mathbf{P}$ be the matrix with columns that are the position vectors $\boldsymbol{p}$ at the receiver locations (whether $\boldsymbol{p}_x$ or $\boldsymbol{p}_y$ is selected depends on the component of the electric field that the receiver picks up). The channel transfer matrix is then $\mathbf{T} = \mathbf{P}^{\mathrm{T}}\mathbf{A}$ and its rank K is bounded by $K \le \min(M, N, L)$. So L limits the number of parallel spatial channels.

Demonstration of capacity analysis for small waveguides: Assume a rectangular waveguide of dimensions $a = 0.7\lambda$, $b = 1.4\lambda$. The allowable modes are: TE: (0, 1), (0, 2), (1, 0), (1, 1); TM: (1, 1).

Fig. 2 shows the capacity of a system with two transmitters and two receivers, under two different kinds of excitation and two sets of receiver locations. Under the first excitation condition, both transmitters excite only the (0, 1) mode with the same power ($K = 1$), and under the second, one transmitter excites the (0, 1) mode and the other one the (0, 2) mode. The two sets of receiver locations are ($y_1 = 0.275\lambda$, $y_2 = 1.125\lambda$) and ($y_1 = 0.275\lambda$, $y_2 = 0.8\lambda$); both receivers are assumed to be on the same z-plane. The first set limits the effective rank of **T**, by using two locations that have the same y-dependence (since we are looking at $(0, n)$ modes, the x-location of the receivers is not significant).

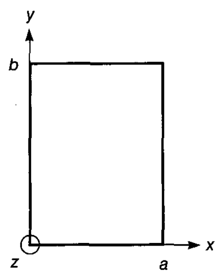

Fig. 1 *Rectangular waveguide*

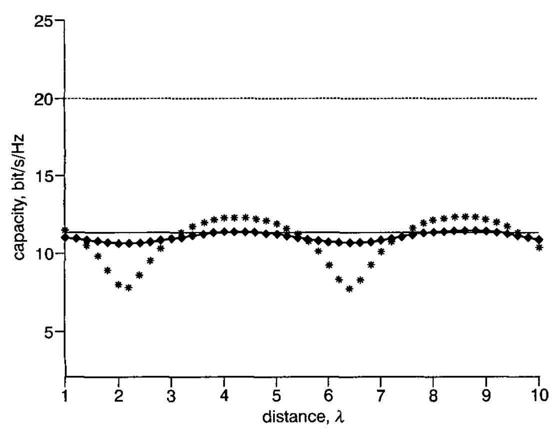

Fig. 2 *Capacity of 2 × 2 system for different excitations and receiver locations*

—— ($y_1 = 0.275\lambda$, $y_2 = 1.125\lambda$), 1 mode
------- ($y_1 = 0.275\lambda$, $y_2 = 0.8\lambda$), 1 mode
* ($y_1 = 0.275\lambda$, $y_2 = 1.125\lambda$), 2 modes
◆ ($y_1 = 0.275\lambda$, $y_2 = 0.8\lambda$), 2 modes

The channel capacity is periodic with z, with the same period for both excitations and receiver locations (for the case of a single excited mode, the capacity is still periodic, but the variation is too small to show in the scale of the axes). The range within which the capacity varies is different because the spread of the eigenvalues of the matrix **T** is different. Exciting a single mode results in poor capacity performance and leads to higher capacity variation with distance. Placing the receivers at locations that have the same y-dependence also limits the rank of the transfer matrix, and therefore the channel capacity. The effects of excitation and location are not separable.

Conclusions: We have analytically shown that the number of allowable propagation modes limits the number of equivalent spatial sub-channels, and demonstrated the dependence of the channel capacity on the excitation, the location of the receivers and the distance along the waveguide.

28 April 2002
Electronics Letters Online No: 20020695
DOI: 10.1049/el:20020695

P. Kyritsi (*Center for PersonKommunikation, Niels Jernes Vej 12, Aalborg Ø, DK-9220, Denmark*)

E-mail: persa@cpk.auc.dk

D.C. Cox (*Stanford University, David Packard Electrical Engineering Building, 350 Serra Mall, Stanford, CA 94305-9515, USA*)

Reference

1 RAMO, S., WHINNERY, J.R., and VAN DUZER, T.: 'Fields and waves in communications electronics' (John Wiley and Sons, Inc, 1994), 3rd edn.

ITU-R total attenuation predictions in comparison with slant path measurements in southern England

S. Ventouras and C.L. Wrench

A simple method to obtain the total attenuation statistics from the statistics of different attenuation effects (gases, clouds, rain) is proposed and tested against measured data along with the current ITU-R methods. The new method based on a rigorous mathematical foundation and experimental observation gives a good agreement with experimental data and highlights the impact of atmospheric gases, cloud and light rain on earth-space systems operating at higher frequencies (Ka/V-band).

Introduction: Efficient design and optimum use of earth-space systems operating above 10 GHz requires the accurate prediction of total attenuation statistics. However, while prediction techniques for estimating the individual tropospheric effects (gases, cloud, rain) have been extensively studied, their statistical combination to obtain the total attenuation remains a difficult problem. This problem is getting harder at higher frequencies (Ka/V-band) where the contributions from light rain, cloud and gases are more severe [1, 2], affecting especially the low fade margin systems.

Recently, four empirical combination methods have been proposed to the ITU-R and evaluated against experimental data [3]. In these methods attenuation levels due to individual tropospheric effects at a given probability level are combined using a variety of root-summed-squared additions to obtain the total attenuation level at the same probability level. Even though it is very convenient from an engineering point of view to combine stochastic variables on equipropable basis, mathematically this is not correct and our measured data indicates that misleading estimates can result.

In this Letter a new method to combine the different attenuation effects is proposed and tested against measured data and the current ITU-R proposed methods. The measurements against which the prediction procedures have been tested in this Letter were collected in southern England using the 18.7, 39.6 and 49.5 GHz beacon signals carried on the geostationary Italian satellite, ITALSAT F1 (elevation angle 30°) [2].

Combination method: Consider two stochastic variables X and Y and their scatter plot on the xy plane (x the horizontal axis). The combined X, Y statistics depend on how the scatter points are distributed on the xy plane. By definition [4] the exceedance probabilities $P(X \geq a)$, $P(Y \geq a)$ and $P(X + Y \geq a)$ for a given threshold a are given by the number of points on the right of line $x = a$, above the line $y = a$ and on the right of line $x + y = a$, respectively, divided by the total number of scatter plot points.

Bearing in mind that in beacon attenuation measurements it is difficult to distinguish rain attenuation from its associated raining–cloud attenuation and as a consequence rain prediction models include also non-raining–cloud attenuation, the combined attenuation due to rain and cloud ($A_{rain+cloud}$) can be written as the sum of two components; the rain and raining–cloud attenuation component (A_{rain}) and the non-raining–cloud attenuation component (A_{cloud}). This implies a (A_{rain}, A_{cloud}) scatter plot which gives:

$$P(A_{rain+cloud} \geq a) = P(A_{rain} \geq a) + P(A_{cloud} \geq a) \qquad (1)$$